Magnetic Desaturation of a Momentum Bias System

K.L. Lebsock*
RCA Astro-Electronics, Redondo Beach, California

A simple observer and controller has been formulated for a low bandwidth yaw attitude control loop on a synchronous orbit momentum bias spacecraft. Operation of the system is entirely autonomous, with the only external reference required being a measurement of the spacecraft roll attitude. Low-level torque actuation is provided by a single magnetic coil that is mounted in the spacecraft body at an arbitrary orientation in the roll/yaw plane. This control system design provides much better pointing accuracy and rate stability for a given bias momentum than previous techniques. Simulated performance during a magnetic storm is presented for a Vee-Wheel momentum bias configuration. The properties of the geomagnetic field at synchronous altitude that are pertinent to spacecraft attitude control system design are described in the Appendix.

Introduction

A UNIQUE magnetic desaturation system has been formulated specifically to meet the yaw rate stability requirements of a Vee-Wheel momentum bias stabilized spacecraft operating in synchronous orbit. The Vee-Wheel configuration of two reaction wheels provides a large momentum bias along the pitch axis for yaw restraint and a smaller yaw component of momentum for roll control and nutation damping (see Fig. 1). This configuration, normally including a small yaw wheel for redundancy, provides two axes of momentum storage capability. It is therefore dynamically equivalent to the orthogonal dual reaction wheel system[1] or the single gimballed wheel system.[2] These systems provide convenient roll offset pointing capability, rapid nutation damping, and, in general, yield better pointing accuracy with less thruster activity than the single-axis (pitch) momentum storage systems derived from WHECON.[3] Two-axis momentum storage systems are used on the synchronous spacecraft TDRSS and INSAT.

The use of thrusters for unloading the orbit plane component of angular momentum places fundamental limitations on the pointing accuracy and rate stability of both one- and two-axis momentum storage systems.[4] The attitude transient produced by an unloading pulse is the dominant roll pointing error in the Vee-Wheel system because the yaw component of the reaction wheel control torque is limited by the sine of the cant angle.[5] The yaw pointing error and long-term rate stability are dominated by the orbit rate interchange of momentum between the wheels and the yaw attitude during the intervals between unloading pulses. These sources of roll and yaw pointing errors can be eliminated by utilizing a magnetic torquer with its dipole axis in the roll/yaw plane. The quiet-day magnetic field at geosynchronous altitude is nominally perpendicular to the orbit plane and is therefore favorably oriented to provide roll and yaw control torques (see Fig. 2). The interaction with the Earth's magnetic field can produce control torques that continuously compensate for the environmental disturbance torques and unload the roll/yaw angular momentum. When considered in this fashion, the magnetic torquing loop is simply a very low bandwidth yaw attitude controller.[6]

Presented as Paper 82-1468 at the AAS/AIAA Astrodynamics Conference, San Diego, Calif., Aug. 9-11, 1982; submitted Aug. 11, 1982; revision received March 22, 1983.

*Manager, Program Development. Member AIAA.

The control torque $\bar{T}_c$ in newton-meters produced by a magnetic torquer is

$$\bar{T}_c = 10^{-9}\bar{m}\times\bar{B} \tag{1}$$

where $\bar{m}$ is the magnetic dipole moment of the torquer in amp-turn-square meters and $\bar{B}$ is the ambient magnetic field strength in gammas ($1\gamma = 10^{-5}$ G). Representative solar radiation pressure torques on synchronous communications satellites are on the order of 10^{-5} N-m. Since the average field strength at synchronous altitude is 110γ the size of the control torquer is typically a few hundred amp-turn-square meters. Detailed sizing considerations are given in the Appendix.

Previous magnetic desaturation systems have used deadband, on-off, or proportional type controllers operating on the roll attitude error signal and/or the wheel tachometer signals.[7] The advent of reliable space qualified microprocessors makes possible the application of observer theory to the design of more efficient and accurate magnetic desaturation systems. This paper describes a simple three-state observer that provides remarkably accurate estimates of the yaw attitude and the roll and yaw environmental torques. The inputs to the observer for the Vee-Wheel configuration are the roll attitude error signal provided by a horizon sensor and the wheel speed tachometer signals. The bandwidth of the observer is chosen to track only those components of the environmental torque that are of significance to the attitude motion of a specific spacecraft configuration. The outputs of the observer are combined in a linear state feedback control law to drive the single body mounted desaturation magnet. Gains for the control law are selected to minimize either the momentum storage requirement of the wheels or the amplitude of the yaw attitude excursion. The observer and control law designs are presented in a generalized momentum format so that their applicability to other types of momentum bias systems is evident. In particular, the control law is shown to be a generalized WHECON type of controller that permits the torquer to be physically mounted at any arbitrary orientation in the roll/yaw plane. The removal of this traditional torquer orientation constraint helps to simplify the task of the spacecraft configuration designer.

The balance of this paper is divided into sections that can be considered independently. In the first section, a generalized magnetic control law for momentum bias systems is developed. This is followed by a section that describes a three-state observer design for a Vee-Wheel configuration that provides estimates of yaw attitude, roll disturbance torque, and yaw disturbance torque. The third major section presents a specific magnetic desaturation system design and simulation results showing its anticipated performance during magnetic

storms. Conclusions are then presented that point out the applicability of these design techniques to other momentum bias systems. Finally, in the Appendix, the Earth's magnetic field at synchronous altitude is characterized as a source of control torque and guidelines are given for the design of magnetic torquers.

Control Law

The satellite control axes (body frame X, Y, Z, in Fig. 1) are central principal axes and nominally aligned with the orbital axes (orbit frame X_0, Y_0, Z_0). The orbit frame rotates in inertial space at the constant orbit rate ω_0 about the $-Y_0$ axis which is normal to the orbit plane. The X_0 axis is in the direction of the satellite's velocity, and the Z_0 axis is directed along the radius vector from the spacecraft to the center of the Earth. The orientation of the body frame is related to the orbital frame by the ordered sequence of Euler angles ϕ (roll), θ (pitch), and ψ (yaw). The angular momentum vector of the rotating components is nominally directed along the negative Y axis with a nominal bias value of H_n for a momentum bias system.

Consider the roll/yaw dynamics of the Earth oriented body expressed in the orbital reference frame. Assume that the spacecraft is controlled so that both the Euler angles and their time derivatives are small. The subscript 0 will be dropped in the following discussion as a matter of convenience. Let H_x and H_z denote the body's angular momentum components in the orbit plane. Let M_x and M_z denote the orbit plane components of the environmental disturbance torques. The magnetic torquer produces a control torque of magnitude T_c at an angle δ from the $+X$ axis in the roll/yaw plane of the body (see Fig. 3).

Since the roll/yaw plane is nearly coplanar with the orbit plane, the equations of motion are approximately given by

$$\begin{bmatrix} S & -\omega_0 \\ \omega_0 & S \end{bmatrix} \begin{bmatrix} H_x \\ H_z \end{bmatrix} = \begin{bmatrix} M_x + T_c\cos\delta \\ M_z - T_c\sin\delta \end{bmatrix} \tag{2}$$

where S is the Laplace operator. Assume the existence of perfect measurements or estimates $\hat{H}_x$ and $\hat{H}_z$ of the angular momenta and $\hat{M}_x$ and $\hat{M}_z$ of the disturbance torques. Let the control torque be proportional to the disturbance torques and a component $\hat{H}_s$ of the angular momentum that is located at an angle γ from the $+Z$ axis, as shown in Fig. 3.

$$\hat{H}_s = \hat{H}_x\sin\gamma + \hat{H}_z\cos\gamma \tag{3}$$

$$T_c = K\omega_0\hat{H}_s + G_x\hat{M}_x + G_z\hat{M}_z \tag{4}$$

The traditional WHECON angle α can be identified as the angle between the control torque $\bar{T}_c$ and an axis that is orthogonal to the sensed momentum $\hat{H}_s$. This angle is chosen to provide damping to the orbit rate roots of the system. The traditional WHECON angle is constrained by the mechanical alignment of the control torquer with the horizon sensor which provides a measure of the yaw component of momentum ($\gamma = 0$). The use of an observer to provide an estimate of the momentum component at any desired angle in the roll/yaw plane permits the selection of a generalized WHECON angle for any arbitrary orientation of the control torque vector. Let the generalized WHECON angle be defined as

$$\alpha = \delta - \gamma \tag{5}$$

where δ is the control torque offset angle and γ is the momentum offset angle. Then the characteristic equation of the controlled satellite can be expressed as

$$S^2 + S\omega_0 K\sin\alpha + \omega_0^2(1 + K\cos\alpha) = 0 \tag{6}$$

Taking $K > 0$, the conditions for stability require that the WHECON angle lies in the range

$$0 < \alpha < \cos^{-1}(-1/K) \tag{7}$$

For the special case of critically damped roots, the momentum gain becomes

$$K = 2/(1 - \cos\alpha) \tag{8}$$

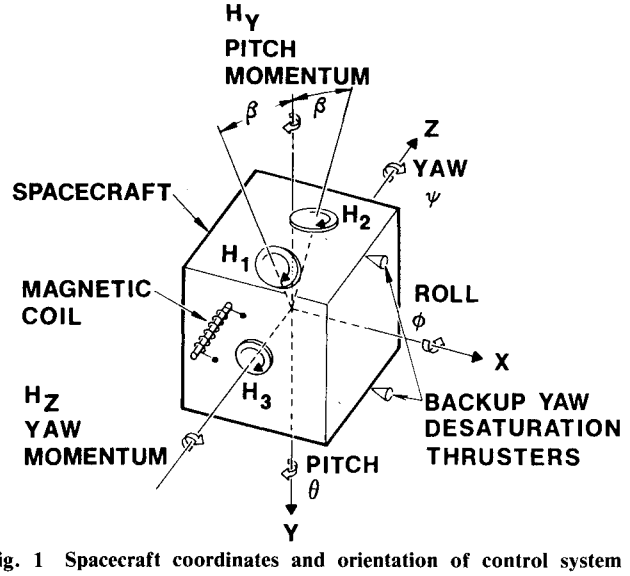

Fig. 1 Spacecraft coordinates and orientation of control system components.

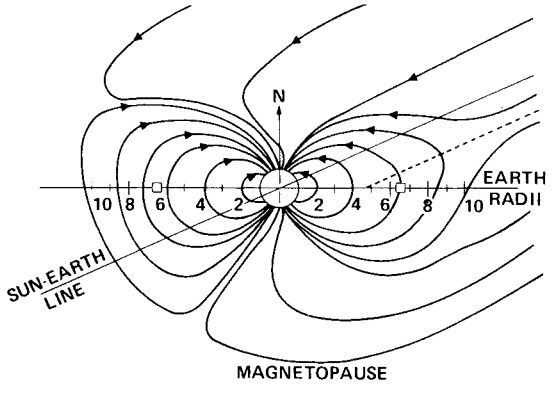

Fig. 2 Earth's magnetic field at winter solstice; squares indicate synchronous altitude (after Ref. 10).

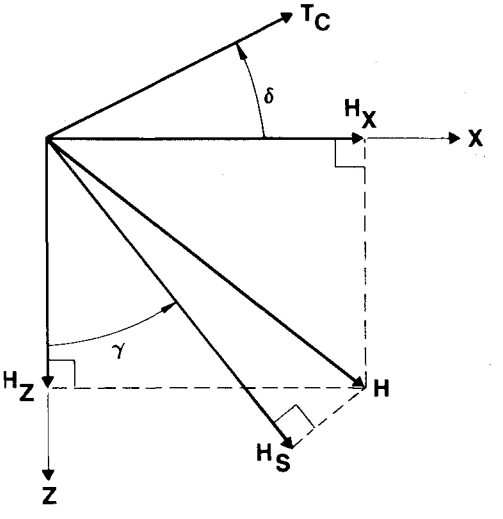

Fig. 3 Spacecraft angular momentum components and magnetic control torque orientation.

and the critically damped natural frequency of the controlled body is

$$\omega_n = \omega_0 \sqrt{\frac{1+\cos\alpha}{1-\cos\alpha}} \tag{9}$$

The traditional WHECON system provides damping of the low-frequency roots by the offset angle α. It also provides control of the nutation roots, which are normally at a higher frequency, by the inclusion of a lead term or derived rate in the horizon sensor error signal. In this paper, it is assumed that nutation damping is provided separately, for example, by the Vee-Wheel momentum control law. However, nutation control could be directly included in the magnetic control law if desired. It should be noted that the form of control law given by Eq. (4) is a WHECON law only in the sense that it provides damping of the low-frequency roots. Here the damping is provided by the momentum gain K, which is related by Eq. (8) to the angle α in the traditional system. The magnetic control law given here also contains torque gains G_x and G_z, which are chosen to shape the momentum response to a particular form of environmental disturbance torque.

The transfer functions relating the roll and yaw momenta to the environmental disturbance torques are found by inverting the controlled system's dynamics matrix as

$$\begin{bmatrix} H_x \\ H_z \end{bmatrix} = \frac{1}{\Delta} \begin{bmatrix} S+K\omega_0\cos\gamma\sin\delta & \omega_0(1+K\cos\gamma\cos\delta) \\ -\omega_0(1+K\sin\gamma\sin\delta) & S-K\omega_0\sin\gamma\cos\delta \end{bmatrix} \times \begin{bmatrix} 1+G_x\cos\delta & G_z\cos\delta \\ -G_x\sin\delta & 1-G_z\sin\delta \end{bmatrix} \begin{bmatrix} M_x \\ M_z \end{bmatrix} \tag{10}$$

where

$$\Delta = S^2 + S\omega_0 K\sin\alpha + \omega_0^2(1+K\cos\alpha) \tag{11}$$

The controller gains can now be selected to produce a desired momentum response to a given disturbance torque history. A common disturbance torque is that of a constant inertially fixed solar torque M_I which is resolved in the orbit frame as

$$M_x = M_I\cos\omega_0 t \tag{12}$$

$$M_z = -M_I\sin\omega_0 t \tag{13}$$

Substituting these forcing functions into the inverted dynamics matrix and solving for the steady-state amplitudes of the resulting momenta excursions at orbit frequency yields

$$|H_x|_{ss} = \frac{M_I}{\omega_0 K}\{(2+K\cos\gamma\cos\delta+G_x\cos\delta-G_z\sin\delta)^2 + (K\cos\gamma\sin\delta-G_x\sin\delta-G_z\cos\delta)^2\}^{1/2} \tag{14}$$

$$|H_z|_{ss} = \frac{M_I}{\omega_0 K}\{(2+K\sin\gamma\sin\delta+G_x\cos\delta-G_z\sin\delta)^2 + (K\sin\gamma\cos\delta+G_x\sin\delta+G_z\cos\delta)^2\}^{1/2} \tag{15}$$

One constrained case that is of particular interest for a dual spinner is that of equal steady-state amplitudes of the roll and yaw momenta. The torque gains required to produce equal momentum amplitudes are

$$G_x = -2\cos\delta - (K/2)\cos(\alpha+\delta) \tag{16}$$

$$G_z = 2\sin\delta + (K/2)\sin(\alpha+\delta) \tag{17}$$

which yield the momentum amplitudes as

$$|H_x|_{ss} = |H_z|_{ss} = M_I/2\omega_0 \tag{18}$$

A second constrained case that is of practical importance, since it tends to minimize yaw attitude excursions, is for the roll momentum amplitude to be set identically to zero. The torque gains required for this case are

$$G_x = -2\cos\delta - K\cos\gamma\cos 2\delta \tag{19}$$

$$G_z = 2\sin\delta + K\cos\gamma\sin 2\delta \tag{20}$$

which give the momentum amplitudes as

$$|H_x|_{ss} = 0 \qquad |H_z|_{ss} = M_I/\omega_0 \tag{21}$$

This last case will be used in selecting gains for the numerical example that is presented in a later section.

The two sets of torque gains G_x and G_z given above have been selected to produce two distinct types of momentum response to a constant, inertially fixed torque. Similar techniques can be utilized to select gains if the disturbance torque contains a large term at some multiple of orbit frequency. For example, the solar radiation pressure torque on a large Earth oriented antenna reflector often results in a significant disturbance torque at twice orbit frequency. The gains G_x and G_z can be selected to produce a desired momentum response to this second harmonic term. Another common case that is of practical concern is the response due to a constant roll bias torque. The roll bias torque on Intelsat V due to solar radiation pressure at the solstices is an example of this situation. Once again the gains can be selected to produce a desired response to this disturbance. This has not been done in the case of the Vee-Wheel system because the roll attitude control loop automatically biases the yaw component of the wheel momentum to counterbalance the roll bias disturbance torque.

State Observation

The control law proposed in the last section requires measurements or estimates of the spacecraft's angular momenta and disturbance torques. The Z_0 component of the Vee-Wheel system's angular momentum is given approximately by

$$H_z = \mathrm{H}_z + \mathrm{H}_y\phi \tag{22}$$

where H_y and H_z are the pitch and yaw components of the wheel's momentum as measured by the tachometers, and ϕ is the roll attitude as measured by the horizon sensor. The X_0 component of the angular momentum is not directly available from measurements, since no continuous yaw attitude measurements are provided by the stationkeeping sun sensor. Consequently, it is necessary to estimate H_x along with M_x and M_z.

Assuming that the dominant environmental disturbance torque is a constant, inertially fixed torque of the form given by Eqs. (12) and (13), the controlled plant equations of motion can be expanded to include this model of the disturbance torque in the form

$$\begin{bmatrix} SH_x \\ SH_z \\ SM_x \\ SM_z \end{bmatrix} = \begin{bmatrix} 0 & \omega_0 & 1 & 0 \\ -\omega_0 & 0 & 0 & 1 \\ 0 & 0 & 0 & \omega_0 \\ 0 & 0 & -\omega_0 & 0 \end{bmatrix} \begin{bmatrix} H_x \\ H_z \\ M_x \\ M_z \end{bmatrix} + \begin{bmatrix} \cos\delta \\ -\sin\delta \\ 0 \\ 0 \end{bmatrix} T_c \tag{23}$$

Table 1 Spacecraft and environmental parameters

I_x roll moment of inertia	1304 N-m^2
I_y pitch moment of inertia	380 N-m^2
I_z yaw moment of inertia	1413 N-m^2
H_n nominal momentum bias	118 N-m-s
m maximum dipole moment	408 A-Turn-m^2
δ dipole mounting angle	0 deg
B average field strength	107γ
M_x roll bias torque	0.2×10^{-5} N-m
M_z yaw bias torque	-1.1×10^{-5} N-m
M_I inertially fixed torque	2.5×10^{-5} N-m
ω_0 orbit rate	7.292×10^{-5} rad/s

The measurement z provided by the tachometers and horizon sensor is simply

$$z=[0\ 1\ 0\ 0]\,[H_x H_z M_x M_z]^T \tag{24}$$

A three-state reduced order observer of the type popularized by Luenberger[8] can now be constructed. The differential equations for the estimator's auxiliary variables are

$$\frac{dW_1}{dt}=-C_1\omega_0 W_1+W_2+C_1W_3 + (\omega_0+C_1^2\omega_0-C_1C_3-C_2)H_z+(\cos\delta-C_1\sin\delta)T_c \tag{25}$$

$$\frac{dW_2}{dt}=-C_2\omega_0 W_1+(C_2+\omega_0)W_3 + (C_1C_2\omega_0-C_2C_3-C_3\omega_0)H_z-(C_2\sin\delta)T_c \tag{26}$$

$$\frac{dW_3}{dt}=-C_3\omega_0 W_1-\omega_0 W_2+C_3W_3 + (C_1C_3\omega_0+C_2\omega_0-C_3^2)H_z-(C_3\sin\delta)T_c \tag{27}$$

The estimates of the desired variables are obtained from the auxiliary variables by the transformations

$$\hat{H}_x=W_1-C_1H_z \tag{28}$$

$$\hat{M}_x=W_2-C_2H_z \tag{29}$$

$$\hat{M}_z=W_3-C_3H_z \tag{30}$$

The characteristic equation of the observer is

$$S^3+S^2(C_1\omega_0-C_3)+S(\omega_0^2+2C_2\omega_0)+\omega_0^2(C_3+C_1\omega_0)=0 \tag{31}$$

where the gains C_1, C_2, and C_3 are selected to provide the desired roots for the estimation process. This observer design is used in the numerical example that is presented in the next section because the disturbance torque histories for that particular spacecraft are well represented by Eqs. (12) and (13).

In general, the disturbance torque histories over the mission lifetime of a particular spacecraft must be carefully examined before a suitable model of them can be selected. The torque model is then used to augment the equations of motion (2) to produce controlled plant equations analogous to Eq. (23) from which an observer can be constructed. Inclusion of terms in the torque model beyond the second harmonic is not necessary for current commercial communications satellite applications. The inclusion of a roll bias torque in the model simply requires the addition of a single state equation that specifies that the derivative of the roll bias torque is zero. The yaw bias torque is unobservable if there is no measurement of absolute yaw attitude. A constant yaw bias torque cannot be estimated as easily for a three-axis body stabilized design as it can for a dual spinner. The spinning sun sensor on a dual spinner provides a simple measurement for yaw attitude determination.

It is worth noting that the primary reference of this class of estimators is the orientation of the momentum bias vector with respect to the orbit normal. Consequently, it is possible to estimate the roll horizon sensor bias provided that the bias momentum is large enough. This fact is of significance to dual spinner type spacecraft, where the payload is normally aligned directly to the despin bearing axis rather than to the horizon sensor.

Numerical Example

The controller and observer developed in the preceding sections are now applied to a Vee-Wheel attitude control system that is designed for the synchronous orbit environment. The physical properties of the spacecraft and the approximate environment are summarized in Table 1. The actual environmental disturbance torque truth model contains terms through the seventh harmonic. The magnetic torquer selected for this spacecraft is a 408 A-turn-m^2 aluminum wire air core coil mounted with the dipole axis parallel to the yaw axis. The magnetic dipole moment strength was selected to provide nearly bang-bang control of a 2.0×10^{-5} N-m inertially fixed torque in a 70γ field. Backup yaw desaturation thrusters are provided that supply minimum bit pulses of 0.083 N-m-s whenever the yaw component of the wheel momentum exceeds 0.65 N-m-s.

An equivalent WHECON angle of 45 deg was selected to provide broad stability margins and a critically damped controller natural frequency of approximately 2½ times orbit rate. From Eq. (8), the momentum gain is found to be $K=6.828$. Since the magnetic coil was designed to mount flush on the periphery of the antinadir face the torquer offset angle is $\delta=0$ deg, and by Eq. (5), the momentum offset angle is $\gamma=-45$ deg. In order to minimize the yaw attitude excursions due to a constant, inertially fixed torque, the torque gains were determined from Eqs. (19) and (20) to be $G_x=6.828$ and $G_z=0.0$. The observer gains of $C_1=7.0$, $C_2=4.02\times10^{-4}$, and $C_3=7.31\times10^{-5}$ were selected from Eq. (31) to provide a real root at 1.64 ω_0 and a complex pair at 2.18 ω_0 with a damping ratio of 0.986. The observer roots were chosen to be approximately equal to those of the controller to insure timely control of disturbance torques but still low enough in frequency to filter out spurious disturbances in the magnetic field. Observer roots faster than four times orbit rate were found to seriously degrade yaw pointing performance during magnetic storms.

The component of the Earth's magnetic field that is normal to the orbit plane is shown in Fig. 4a. The history extends over a 4-day period, with time being measured from midnight. Around dusk of the first day a large magnetic storm begins that results in the collapse of the field for almost half a day. During this period the magnetic coil is ineffective and the backup desaturation thrusters are pulsed four times at ½-h intervals.

The roll and yaw environmental disturbance torques are shown by solid lines in Figs. 4b and 4c, respectively. This environmental torque is produced by solar radiation pressure at the solstice when the spacecraft's center of pressure is north of the orbit plane. The estimated environmental torque generated by the first harmonic model in the observer is shown by the dashed lines. On magnetically quiet days the estimated environmental torques follow the actual torques with reasonable accuracy up to the second harmonic due to the selection of the eigenvalues. The discrepancy between the actual and estimated torques during the magnetic storm is caused by the large error in the control torque that is fed back into the observer. The control torque T_c is computed using an assumed constant magnetic field strength of 107γ. Some

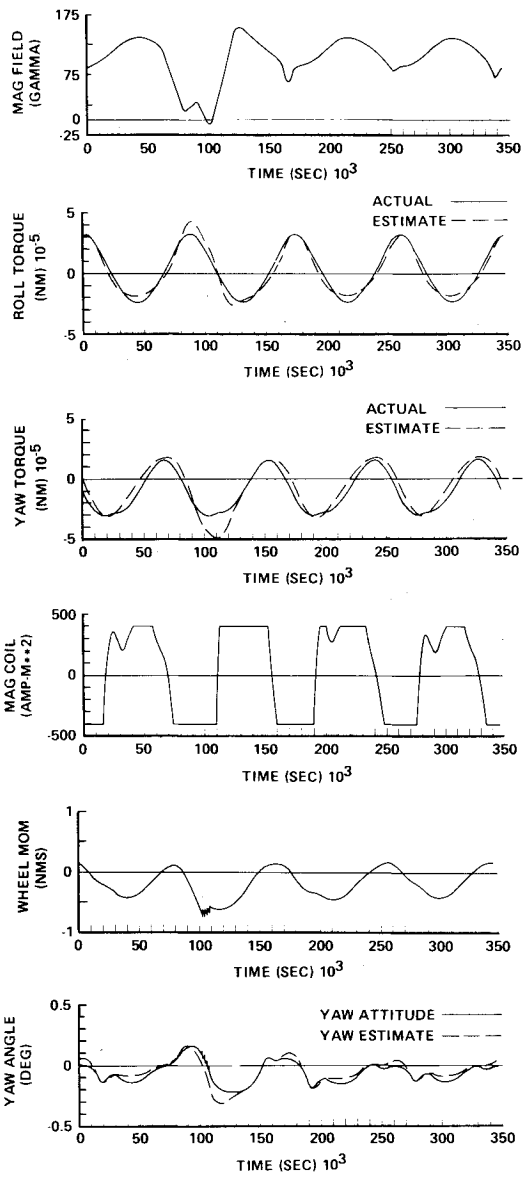

Fig. 4 a) Ambient magnetic field, $-B_y$. b) Roll environmental torque, M_x. c) Yaw environmental torque, M_z. d) Magnetic coil dipole moment, m. e) Yaw wheel momentum, H_z. f) Spacecraft yaw attitude, ψ.

improvement in performance could be obtained by adding a diurnal sinusoidal component to the field model that is used to compute the control torque. The addition of a pitch axis magnetometer could remove all of the errors due to the time variations in the field strength. However, in most applications this additional hardware is not warranted.

The magnetic dipole moment produced by the coil is shown in Fig. 4d. Note that the magnetic coil operates in a highly saturated mode because the actual disturbance torque level is 25% higher than the design value. During the magnetic storm the coil operates in a totally saturated or bang-bang mode. The four backup thruster desaturation pulses are fired to augment the magnetic coil torque as the ambient magnetic field strength approaches zero. The inputs to the observer are held constant for 300 s following each of the thruster pulses so that the state estimates are not perturbed by the transients produced by the pulses. This period was chosen because it is sufficiently long to permit the wheel speed control loop to damp out nutation and restore roll attitude to less than 0.01 deg accuracy.

Nearly all of the spacecraft's yaw axis component of angular momentum is stored in the wheels. The yaw component of the wheel momentum is shown in Fig. 4e. The 0.34 N-m-s amplitude of the momentum oscillation is consistent with that predicted by Eq. (21). The spacecraft's roll axis component of angular momentum is stored in the yaw attitude, ay shown in Fig. 4f. The unobservable yaw bias torque results in a constant negative yaw attitude offset of nearly 0.07 deg. The distorted yaw oscillation about this bias level is due to the simplified dynamics model used in the observer and the nonlinear operation of the magnetic controller. Note that the firing of the yaw desaturation thrusters does change the yaw wheel momentum by 0.083 N-m-s per pulse, but leaves the yaw attitude unchanged after the transient has subsided.

Conclusions

The three-state observer provides useful estimates of the yaw attitude and roll and yaw disturbance torques for a specific class of momentum bias stabilized spacecraft. These spacecraft have some independent means of nutation damping and are subjected to an environmental disturbance torque that is approximately constant in inertial space. Two additional states can be added to the observer to provide nutation damping and direct roll attitude control capability. This addition could be particularly desirable for single-axis momentum storage systems. Additional states may also be added to more accurately model the environmental disturbance torque as required. The addition of second harmonic environmental torque terms may be of importance for spacecraft with very large antenna reflectors.

The control law developed for a single, body mounted, magnetic dipole utilizes both the estimated momentum and the disturbance torque. The momentum gain and the momentum offset angle are selected to produce the desired controller roots. The torque gains are selected to provide a desired momentum response to a constant, inertially fixed disturbance torque. Similar design techniques can be applied to select torque gains for more complicated disturbance torque histories.

Appendix

The following summary of the main features of the Earth's magnetic field at synchronous altitude and magnetic torquer design considerations is intended as an aid to attitude control engineers who are unfamiliar with this field. Research into the details of the magnetic field has produced a large and rapidly growing body of scientific literature. For example, the 1979 survey paper by McPherron[9] on magnetospheric substorms listed 360 references on this topic alone, and he asserts that an equal number of papers referenced substorms in their title, abstract, or key words in the four preceding years.

Prior to 1957, it was widely assumed that the shape of the Earth's magnetic field was that of a simple dipole much like the field of a bar magnet. Artificial satellite data taken over the past 25 years has established that the shape of the field is significantly affected by the solar wind[10] (see Fig. 2). The magnetic field is compressed on the day side, typically extending 70,000 km toward the sun. It is stretched into an elongated tail that is many millions of kilometers long on the night side. The envelope of the magnetosphere is very dynamic, changing continuously due to solar activity and the relative orientation of sun and Earth.

The quiet-day magnetic field at geosynchronous altitude is roughly perpendicular to the orbit plane and is therefore favorably oriented to provide roll and yaw control torques. The $-Y$ component (geographical north) has an average value of approximately 110γ. The daily variation of this component is typically 30 to 35γ, with the maximum occurring near local noon and the minimum occurring near local midnight. This pattern of diurnal variations in B_y does not exhibit appreciable seasonal effects. The X (geographical east) and Z (nadir) components have biases and daily variations on the order of 10 to 15γ. The form of the B_x and B_z daily variations is strongly dependent on season. These components

also possess slight seasonal asymmetries in their daily ranges, with the range in summer being larger than in winter. The diurnal and seasonal variations are caused by the relative motion of the satellite and the magnetopause, ring, tail, and neutral sheet current systems.[11-13]

The quiet-day model described above has been obtained by averaging spacecraft magnetometer measurements of the five or six quietest days of each month. The most common disturbance to the magnetic environment at synchronous altitude is the magnetic substorm. Magnetic substorms normally occur in the dusk to midnight quadrant and are characterized by a decrease in the field strength and an inclination radially outwards of the magnetic field vector. Substorms typically last from 3 to 5 h and depress the magnitude of the B_y component by 20 to 40γ. Smaller magnitude substorms on the order of 5 to 10γ and lasting for less than 1 h are observable in the quiet-day field model. Consequently, some substorm activity should reasonably be expected to occur on a daily basis. The physical explanation for the existence of magnetic substorms involves the formation and disruption of partial ring currents in the dusk to midnight quadrant. The field lines are stretched in the antisolar direction over a period of several hours and then collapse back within approximately 10 min. This stretching can cause the field direction to change by several tens of degrees at synchronous altitude. Superimposed on this are irregular fluctuations of a few gammas with periods of one to several minutes during a typical substorm.[14]

Magnetic storms are major disruptions in the geomagnetic field induced by solar activity which on rare occasions can result in a temporary reversal of the field at synchronous altitude. Their average frequency of occurrence is on the order of once every three weeks although their frequency may be two or three times greater in years of maximum solar activity. Major magnetic storms occur two or three times more frequently around the equinoxes; however, they can occur during any month and start at any time of day. A typical magnetic storm may last one or two days with the magnitude of B_y being increased on the dayside and decreased on the nightside. The field on the nightside is typically depressed by 30 to 70γ for a period of 3 to 7 h. On occasion, B_x and B_z may exceed B_y in magnitude. In addition, there may be irregular fluctuations in the magnitude of B_y of 10 to 50γ over intervals of 5 min to 2 h, particularly on the nightside. A great magnetic storm that produces a zero or slightly negative B_y component for a period of 1 h may reasonably be expected approximately once per year.[15]

Even more intense storms occur at less frequent intervals. An extremely severe magnetic storm occurred on May 25, 1967. This is one of the ten largest magnetic storms which have occurred since 1932 as measured on the Earth's surface. Coleman presents the ATS 1 and ground based magnetometer records of that storm. The B_y component of the field at ATS 1 displayed an increase in field strength normal to the orbit plane of approximately 80γ over a 2-h period. The field then rapidly changed direction as the magnetopause passed by and remained at a negative magnitude of 80 to 160γ for a period of 3½ h. The field then jumped back to its normal polarity as the magnetopause recrossed the orbit, and stayed at an unusually high level for an additional hour. The next magnetic storm of approximately equal magnitude did not occur until Aug. 28, 1978. A storm of this intensity might be expected once during a typical spacecraft's 7 to 10 year design life.

The time variations in the magnetic field described above can be largely ignored in designing a magnetic desaturation system for a momentum bias spacecraft with a high ratio of angula momentum to environmental disturbance torque. Magnetic systems for high momentum systems, such as the traditional dual spinner, can be designed using the average value of the magnetic field because the precession rate is relatively small. On the other hand, the classical three-axis body stabilized momentum bias spacecraft has a much lower angular momentum to environmental disturbance torque ratio. Consequently, the precession rate is at least one and more often two orders of magnitude larger than that of a dual spinner. In the three-axis case, the spacecraft attitude is more directly affected by the time variations in the ambient magnetic field. The magnetic torquer must, therefore, be designed to operate in a lower effective magnetic field. The magnetic torquer for a three-axis spacecraft will typically be designed for a magnetic field strength of 70γ, depending, of course, upon the pointing accuracy required of the system.

The controller's magnetic dipole moment can be produced by either an air core or an iron core coil. It is readily shown that iron core magnets have a smaller weight times power product than air core magnets. This would appear to make iron core magnets the natural choice for satellite attitude control.[16] However, the air core magnet may still be preferred when such factors are considered as ease of manufacture and integration, magnetic cleanliness when the power is switched off, and the variation in the available power profile over the mission lifetime.

Preliminary sizing of the magnetic torquer is performed by considering the dominant environmental torque M_I to be of constant magnitude and perpendicular to the sunline. Complete compensation of the environmental torque could be achieved by providing a control torque T_c of strength M_I mounted on a sun tracking solar array. However, system integration constraints frequently require that the magnetic torquer be mounted on the Earth oriented segment of the satellite. The only spacecraft that have been considered in this paper are those that are controlled by a magnetic torquer that is body mounted on the Earth oriented segment. Here the magnetic torquer must be sized at $2M_I$ to provide linear control or $(\pi/2)M_I$ to provide bang-bang control. In both the linear and saturated controller cases, the operation of the body mounted magnetic torquer will produce cyclical angular momentum excursions as it provides compensation for the environmental torque.

Acknowledgment

The three-state observer described in this paper was originally designed in 1978 for the INSAT spacecraft at the Western Development Laboratories of Ford Aerospace and Communications Corporation.

References

[1]Terasaki, R., "Dual Reaction Wheel Control of Spacecraft Pointing," Symposium on Attitude Stabilization and Control of Dual Spin Spacecraft, El Segundo, Calif., SAMSO and Aerospace Corp., Aug. 1967.

[2]Broquet, J., "Attitude Stabilization of Geostationary Satellite with a Single Degree of Freedom Angular Momentum Wheel System," VII IFAC Symposium on Automatic Control in Space Preprints, Vol. 2, May 1976.

[3]Dougherty, H.J., Scott, E.D., and Rodden, J.J., "Analysis and Design of WHECON – An Attitude Control Concept," AIAA Paper 68-461, San Francisco, Calif., April 1968.

[4]Lebsock, K.L., "High Pointing Accuracy with a Momentum Bias Attitude Control System," *Journal of Guidance and Control,* Vol. 3, May-June 1980, pp. 195-202.

[5]Markland, C.A., "A Review of the Attitude Control of Communications Satellites," IAF Paper 81-344, Rome, Italy, Sept. 1981.

[6]Schmidt, G.E. Jr. and Muhlfelder, L., "The Application of Magnetic Torquing to Spacecraft Attitude Control," AAS Paper 81-002, Keystone, Colo., Feb. 1981.

[7]Dougherty, H.J., Lebsock, K.L., and Rodden, J.J., "Attitude Stabilization of Synchronous Communications Satellites Employing

Narrow-Beam Antennas," *Journal of Spacecraft and Rockets,* Vol. 8, Aug. 1971, pp. 834-841.

[8]Bryson, A.E. Jr. and Luenberger, D.G., "The Synthesis of Regulator Logic Using State-Variable Concepts," *Proceedings of the IEEE,* Vol. 58, Nov. 1970, pp. 1803-1811.

[9]McPherron, R.L., "Magnetospheric Substorms," *Reviews of Geophysics and Space Physics,* Vol. 17, June 1979, pp. 657-681.

[10]Cummings, W.D., Barfield, J.N., and Coleman, P.J. Jr., "Magnetospheric Substorms Observed at the Synchronous Orbit," *Journal of Geophysical Research, Space Physics,* Vol. 73, Nov. 1968, pp. 6687-6698.

[11]Coleman, P.J. Jr. and Cummings, W.D., "Stormtime Disturbance Fields at ATS 1," *Journal of Geophysical Research,* Vol. 76, Jan. 1971, pp. 51-62.

[12]Olson, W.P. and Cummings, W.D., "Comparison of the Predicted and Observed Magnetic Field at ATS 1," *Journal of Geophysical Research, Space Physics,* Vol. 75, Dec. 1970, pp. 7117-7121.

[13]Cummings, W.D., Coleman, P.J. Jr., and Siscoe, G.L., "Quiet Day Magnetic Field at ATS 1," *Journal of Geophysical Research,* Vol. 76, Feb. 1971, pp. 926-932.

[14]Vasyliunas, V.M., "An Overview of Magnetospheric Dynamics," *Magnetospheric Particles and Fields,* edited by B.M. McCormac, D. Reidel Publishing Co., Boston, 1976, pp. 99-110.

[15]Chernosky, E.J. and Maple, E., "Geomagnetism," *Handbook of Geophysics,* The Macmillan Co., New York, 1960, Chap. 10, pp. 1-8.

[16]Mesch, F., "Magnetic Components for the Attitude Control of Space Vehicles," *IEEE Transactions on Magnetics,* Vol. 5, Sept. 1969, pp. 586-592.